TISSUE ENGINEERING: Part A
Volume 20, Numbers 23 and 24, 2014

DOI: 10.1089/ten.tea.2013.0729

Improved Peripheral Nerve Regeneration Using Acellular Nerve Allografts Loaded with Platelet-Rich Plasma

Canbin Zheng, MD, PhD,[1] Qingtang Zhu, MD, PhD,[1] Xiaolin Liu, MD, PhD,[1] Xijun Huang, MD,[1] Caifeng He, MD,[2] Li Jiang, PhD,[3] and Daping Quan, PhD[4]

Acellular nerve allografts (ANAs) behave in a similar manner to autografts in supporting axonal regeneration in the repair of short peripheral nerve defects but fail in larger defects. The objective of this article is to evaluate the effect of ANA supplemented with platelet-rich plasma (PRP) to improve nerve regeneration after surgical repair and to discuss the mechanisms that underlie this approach. Autologous PRP was obtained from rats by double-step centrifugation and was characterized by determining platelet numbers and the release of growth factors. Forty-eight Sprague–Dawley rats were randomly divided into 4 groups (12/group), identified as autograft, ANA, ANA loaded with PRP (ANA + PRP), and ANA loaded with platelet-poor plasma (PPP, ANA + PPP). All grafts were implanted to bridge long-gap (15 mm) sciatic nerve defects. We found that PRP with a high platelet concentration exhibited a sustained release of growth factors. Twelve weeks after surgery, the autograft group displayed the highest level of reinnervation, followed by the ANA + PRP group. The ANA + PRP group showed a better electrophysiology response for amplitude and conduction velocity than the ANA and ANA + PPP groups. Based on histological evaluation, the ANA + PRP and autograft groups had higher numbers of regenerating nerve fibers. Quantitative real-time polymerase chain reaction (qRT-PCR) demonstrated that PRP boosted expression of neurotrophins in the regenerated nerves. Moreover, the ANA + PRP and autograft groups showed excellent physiological outcomes in terms of the prevention of muscle atrophy. In conclusion, ANAs loaded with PRP as tissue-engineered scaffolds can enhance nerve regeneration and functional recovery after the repair of large nerve gaps nearly as well as autografts.

Introduction

Peripheral nerve injuries cause morbidity in ~2.8% of all trauma patients, leaving many with long-term disabilities with high societal costs.[1] The gold standard of treatment for a peripheral nerve defect is the implantation of an autologous nerve graft, which currently offers the best outcome for patients. However, autograft repair is limited by the availability of donor tissue, the need for extra incisions, the sacrifice of a donor nerve, and size mismatching.[2] As a result, the development of an effective alternative graft material is desirable.

Various materials have been used to fabricate nerve conduits, with many attempts at improvement. The ideal graft material should have physical and biochemical characteristics similar to those of the native nerve.[3] To avoid the problems of graft availability, donor site morbidity, and immune rejection, acellular nerve allografts (ANAs) are highly promising nerve autograft substitutes obtained by the chemical extraction of native peripheral nerve tissues. The extraction process reduces graft immunogenicity by eliminating cellular constituents, while the regenerative capacity is enhanced through the preservation of native extracellular matrix components.[4] The physical and biochemical characteristics of ANAs are similar to those of native nerves, supporting greater numbers of regenerating axons and the more successful guidance of regenerating axons compared with empty conduits.[3,5]

Axonal regeneration in ANAs is similar to that in autografts across short gaps,[6] but is reduced across longer defects, in which unsatisfactory functional recovery is typically achieved due to the lack of an optimal environment for the advancing axonal sprouts.[7] Many studies have demonstrated that the delivery of support cells, such as Schwann cells (SCs) and the inclusion of growth factors within ANAs, as tissue-engineered nerve grafts, improves the regeneration distance and repair speed.[8–10] Early selection of these suitable biological treatments are an ideal way to accelerate nerve regeneration. However, cells therapies are still limited in clinical applications

[1]Department of Orthopedic and Microsurgery, The First Affiliated Hospital, Sun Yat-sen University, Guangzhou, China.
[2]Guangzhou ZhongDa Medical Equipment Co., Ltd., Guangzhou, China.
[3]Orthopedic Institute of The First Affiliated Hospital, Sun Yat-sen University, Guangzhou, China.
[4]School of Chemistry and Chemical Engineering, Sun Yat-sen University, Guangzhou, China.

due to practical disadvantages (e.g., the harvest and culture of the cells, the high risk for potential complications, the costly and time-consuming processing constraints, and various ethical problems).[11,12] Growth factors have been enjoying more popularity in the field of regeneration of the peripheral nerve and many have been proved to be effective.[13] Identification of these growth factors has led to strategies to deliver platelet-derived factors to the axonal sprouting and regeneration.

Platelet-rich plasma (PRP) is an autologous cell therapy containing many bioactive factors that are involved in wound healing and tissue repair, which has several advantages compared with other products and techniques. It can be prepared from autologous blood isolated by puncture as an entirely safe procedure. The clinical use of PRP causes no adverse events or postoperative complication.[14] Meanwhile, the preparation of PRP is rapid, simple, convenient, and economical.[15] Furthermore, PRP provides a high level of a natural variety of growth factors, including platelet-derived growth factor (PDGF), transforming growth factor-β (TGF-β), insulin-like growth factor-1, fibroblast growth factor, epithelial growth factor, and vascular endothelial growth factor, among others.[16] The presence of these growth factors with high concentrations in PRP is directly responsible for increasing cell proliferation, raising collagen production, initiating angiogenesis, and inducing cell differentiation involved in tissue regeneration.[17] PRP-related products are used in various surgical fields to accelerate the healing process after muscle, ligament, joint, and tendon injuries.[18,19] In our previous study, PRP had the potential to stimulate cell proliferation, induced the synthesis of neurotrophic factors, and significantly increased migration of SCs, which indicated that PRP may also provide beneficial therapeutic effects for peripheral nerve regeneration after a nerve injury by supplying growth factors.[20] However, it is still unclear whether the artificial nerve conduits loaded with PRP would be applicable to the reconnection of larger nerve lesions, and whether they would offer long-term beneficial effects for functional recovery of damaged nerves. In addition, to the best of our knowledge, no one has used scaffold ANAs accompanied by PRP to enhance the repair capacity for peripheral nerve injuries. In the present study, we hypothesize that growth factors can be administered with sustained release from PRP gel and that peripheral nerve regeneration can be enhanced after surgical reconstruction by using ANAs enriched with PRP, improving the success of autografts.

Materials and Methods

Animals

Seventy-eight male Sprague–Dawley (SD) rats, weighing ~250–350 g, were provided by Sun Yat-sen University (Guangzhou, Guangdong Province, China). All experimental procedures involving animals were conducted according to the US National institutes of Health guidelines for the care and use of laboratory animals and were approved by the Administration Committee of Experimental Animals of The First Affiliated Hospital of Sun Yat-sen University.

Preparation of ANAs

We used 30 adult SD rats as donors for nerve allografts. The rats were anesthetized by an intraperitoneal injection with ketamine HCl (100 mg/mL). The sciatic nerves (≥2.0 cm in length) were excised from the rats, then cleaned of external fat and connective tissue, and immediately placed in phosphate-buffered saline (PBS) medium. The nerve segments were treated with chemical detergents to remove cellular components as previously described.[21,22] Briefly, the nerve segments were agitated in deionized distilled water for 7 h and treated with 3% (v/v) Triton X-100 (Sigma-Aldrich, St. Louis, MO) overnight, followed by treatment with 4% (w/v) sodium deoxycholate (Sigma-Aldrich) for an additional 24 h. After thorough washing in 10 mM PBS, the nerve segments were sterilized by 12 h irradiation with Co60 (Guangzhou Huada Biological Technology Co., Ltd., Guangzhou, China) and stored in 10 mM PBS at 4°C until use. Harris hematoxylin and eosin (H&E) staining of longitudinal sections and scanning electron microscopy of cross-sections (JSM-6330F; NEC, Tokyo, Japan) were used to examine the characteristics of the acellular nerves as previously described.[4]

Preparation and activation of PRP and platelet-poor plasma

In order to evaluate the characteristics of PRP before animal studies, 11 additional adult SD rats were sacrificed to provide blood for the *in vitro* tests. PRP was prepared by modifying the method of Yamaguchi *et al.*[23] Briefly, 4 mL of fresh blood collected by way of cardiac puncture was mixed with 0.4 mL of 3.2% sodium citrate. The mixture was immediately centrifuged at 400 *g* for 10 min. The supernatant was transferred with a sterile pipette to another tube with a buffy coat and then centrifuged again at 800 *g* for 10 min. The top three-quarters of the supernatant, which consisted of the platelet-poor plasma (PPP), was aspirated and transferred to a new tube. The remaining fraction contained PRP. Approximately 400 μL of either PRP or PPP was activated with 40 μL of 10% calcium chloride solution and 100 U/mL bovine thrombin (Sigma-Aldrich) to form a gel.

The prepared PRP, PPP, and whole-blood aliquots were subjected to platelet counting using a cell counter (Haematology Analyser; Sysmex, Kobe, Japan). The release of PDGF-BB and TGF-β1 from the PRP gels was observed *in vitro*. The PRP gels were immersed in 200 μL PBS (10 mM phosphate, 137 mM NaCl, pH 7.4) in 96-well culture plates and incubated at 37°C with constant agitation. Supernatants were collected at predetermined time points, and the medium was replenished with fresh PBS. All exudates were stored at −80°C for the later measurement of PDGF-BB and TGF-β1 levels using an enzyme-linked immunosorbent assay (ELISA) development kit (R&D Systems, Minneapolis, MN). The immunoassays were performed in duplicate following the manufacturer's instructions.

Surgical procedures and experimental groups

A total of 48 male adult SD rats were randomized into four groups ($n = 12$ each) for the receipt of autografts, ANAs, PRP-treated ANAs (ANA + PRP), or PPP-treated ANAs (ANA + PPP). All surgical procedures were performed by the same surgeon under aseptic operating conditions using ketamine HCl (100 mg/mL) anesthesia. The right sciatic nerve was exposed and transected at a constant point. A chemically extracted 15-mm-long acellular nerve graft with respective experimental content was attached with interrupted microepineurial sutures

to the proximal and distal stumps, which resulted in a 15-mm gap. For the autograft group, a 15-mm-long sciatic nerve was excised, and then reversed 180° and re-implanted. For the ANA group, the sciatic nerve defect was bridged using an ANA only. For the ANA + PRP and ANA + PPP groups, 400 μL of autologous PRP or PPP from the same rat was prepared according to the earlier described methods, and was injected into the mold using a pipette. Then, it was activated with 40 μL of 10% calcium chloride solution and 100 U/mL bovine thrombin to form a solid gel with an at least 15 mm long flat shape. PRP or PPP gel was then wrapped around the ANA surface. To avoid the gel's moving away from the graft, the gel was then fixed around the connective tissue with 8-0 silk sutures. All grafts were sutured to the epineurium of the proximal and distal nerve stumps with 10-0 monofilament nylon sutures under 10× magnification (Olympus SZ61; Olympus, Tokyo, Japan). The left contralateral sciatic nerve served as the positive control.

Functional evaluation of nerve regeneration

Functional recovery was assessed by calculating the sciatic functional index (SFI) value, which is a well-established and commonly used method for the assessment of motor nerve recovery after sciatic nerve injury. The animals were placed in a confined walkway with a dark shelter at the end, as previously described.[24,25] Postoperatively, animals were assessed every 4–12 weeks. The investigators were blinded to the animal treatment groups during walking-track analysis.

Electrophysiological assessment

Eight rats randomly selected from each group were anesthetized, and the injured sciatic nerves were exposed at 12 weeks after surgery. Electrical stimuli were applied to the nerve trunks at the distal or proximal portions of the grafting site, and the compound muscle action potentials (CMAPs) were recorded on the triceps surae muscle belly by using a portable biological function experimental system (BL-420F; TaiMeng, Inc., Chengdu, China). Normal CMAPs were measured from the contralateral uninjured sides. The motor nerve conduction velocity (MCV) was calculated from the derived latencies and the distance between the stimulating and recording electrodes.

Histologic evaluation of regenerated nerves

Following the electrophysiology study, the eight sciatic nerves of each group were excised from the implantation side, and then, the nerves were postfixed. The regenerated nerves were cut into three parts. The middle stump was prepared for histological evaluation, and the distal stump was prepared for immunohistochemical analysis. The contralateral sciatic nerves were used as controls. For each sample, a 1- to 2-mm slice of the regenerated nerve was taken at the middle of the implant. The nerve samples were osmicated, dehydrated, and embedded in Epon. Transverse semi-thin sections (1 μm in thickness) were stained with 1% toluidine blue for morphometric analysis, and ultra-thin sections (50 nm) were used for transmission electron microscopy (TEM; Hitachi H7000, Tokyo, Japan) as previously described.[26] The axons were analyzed as previously described.[27] To determine the axon density based on the total number of myelinated axons, images were captured using a CCD camera (Olympus DP70; Olympus) attached to a microscope system running ImagePro Plus software (Media Cybernetics, L.P., Silver Spring, MD). The axons in each image were counted, and the total number of myelinated axons was calculated for each specimen. The thickness of the myelin sheath and the diameters of the myelinated axons, as well as the G-ratios (the ratio of the axon diameter to the total fiber diameter), were quantified from the TEM images using Image J, the software developed and freely distributed by the US National Institutes of Health. For each specimen, a total of 50–60 random axons were analyzed.

Immunohistochemical analysis

The distal portions of the nerve implants were embedded in paraffin, and 3-μm-thick longitudinal sections were cut using a cryostat (CM3050s; Leica, Wetzlar, Germany), followed by collection on coated slides. The sections were examined by H&E staining to observe the structures of the newly formed nerves. Then, antibodies to neurofilament (NF) and S-100 were used as markers for the axon and myelin sheath. The specimens intended for immunohistochemistry were blocked by a nonspecific immunoreaction; next, the sections were incubated in the solution of NF antibody (1:200 dilution; Sigma-Aldrich) and S-100 protein antibody (1:200 dilution; Santa Cruz Biotechnology, Dallas, TX) for 1 h at room temperature. Subsequently, the sections were incubated in biotinylated anti-mouse rabbit IgG solution for 1 h. Horseradish peroxidase-labeled secondary antibody was developed by the diaminobenzidine method. The quantification of NF and S-100-positive areas was carried out with six randomly selected fields of each specimen. First, a low magnification image (40×) that encompassed the entire regenerated nerve area was captured. The circumference of the nerve was outlined, and the total nerve area was determined. Then, six images (200×) were randomly captured for each nerve specimen, so that at least 40% of the area of regeneration was used for analysis.

Quantitative real-time RT-PCR analysis of gene expression

The gene expression of the markers of axon and neurotrophic factors in all groups ($n = 4$/each) was analyzed using quantitative real-time polymerase chain reaction (qRT-PCR) as previously described.[28,29] Grafts measuring 15 mm in length and ~5 mm of proximal and distal host nerve stumps were harvested. The total RNA was extracted from tissue samples using TRIzol (TaKaRa Biotech, Dalian, China) according to the manufacturer's directions. The RNA concentration was determined via absorbance measurements at 260 and 280 nm using a UV spectrometer (NanoDrop 2000; Thermo Fisher Scientific, Waltham, United Kingdom). The total RNA was then used to synthesize complementary DNA (cDNA) strands by reverse transcription with a PrimeScript RT Reagent Kit (TaKaRa Biotech). cDNA synthesis was performed under conditions of 37°C for 15 min followed by incubation at 85°C for 5 s to terminate the reaction. Rat-specific primers were used for nerve growth factor (NGF), glial-derived growth factor (GDNF), growth-associated protein 43 (GAP43), and neurofilament heavy (NF-H). Glyceraldehyde-3-phosphate dehydrogenase (GAPDH) was used as an internal

control. The forward and reverse primer sequences were designed using Primer Express 2.0 software (Applied Biosystems, Foster City, CA) and synthesized by TaKaRa Biotech. The cDNA samples (2 μL) were amplified in triplicate using real-time PCR in a final volume of 20 μL using SYBR Premix Ex Taq (TaKaRa Biotech) following the manufacturer's instructions. All qRT-PCR experiments were performed using an iQ5 Real-Time Detection System (Bio-Rad, Richmond, CA). The cDNA was amplified under conditions of 30 s at 95°C, followed by 40 cycles of 5 s at 95°C and 30 s at 60°C, with data collection performed during the final 30 s. A final melting curve analysis was performed to distinguish the main PCR products from primer dimers. The fold changes in gene expression relative to the control (ANA group) were calculated using $2^{-\Delta\Delta Ct}$. All experimental samples were assayed in triplicate.

Weight, tension, and morphometric examination of the triceps surae muscles

Before the excision of the nerve implant, the triceps surae muscles from both the experimental and control sides were dissected and detached from the bone at their distal insertion. For each muscle, the terminal point was then connected to a muscle tension transducer (BL-420F biological function experimental system; TaiMeng, Inc.) using a 3-0 nylon suture thread. The maximum muscle contraction tension was then recorded. The muscle tension on the side of the operation was expressed as a percentage of the control side. Finally, the bilateral triceps surae muscles were completely dissected from their insertion points, removed, and immediately weighed. The conservation muscle-mass ratio was recorded as the ratio of the muscle weight of the contralateral normal side.

A small piece measuring $5 \times 5 \times 5$ mm of each of the triceps surae muscle samples was mounted in O.C.T compound (Sakura, Tokyo, Japan), and transverse sections (50 μm in thickness) were cut on a cryostat (Leica, Richmond, IL). Acetylcholinesterase (AChE) cytochemical staining with alpha-banded krait venom was used for fluorescence microscopy visualization (Olympus DP70; Olympus). The remaining muscle samples were fixed in 4% (v/v) formaldehyde and cut on a cryostat into transverse sections, which were subjected to Masson trichrome staining followed by observation under light microscopy. Photographs were collected from four randomly selected fields in each specimen and were analyzed with Image-Pro plus software to measure the cross-sectional area of the muscle fibers. The percentage of collagen fibers was calculated by dividing the collagen fiber area by the collagen fiber and muscle fiber area.

Statistics

The statistical procedures were carried out using SPSS 15.0. software package for Windows (SPSS, Inc., Chicago, IL). The data are expressed as the mean values ± standard deviation. Statistical analysis was performed with a one-way analysis of variance to determine the significant differences among four groups. Intergroup statistical differences were examined by the Bonferroni multiple-comparison test. Values of $p < 0.05$ were considered statistically significant.

Results

The structure of the acellular nerve grafts

After chemical extraction, H&E staining showed that no cells, including SCs, endothelium cells, blood cells, and

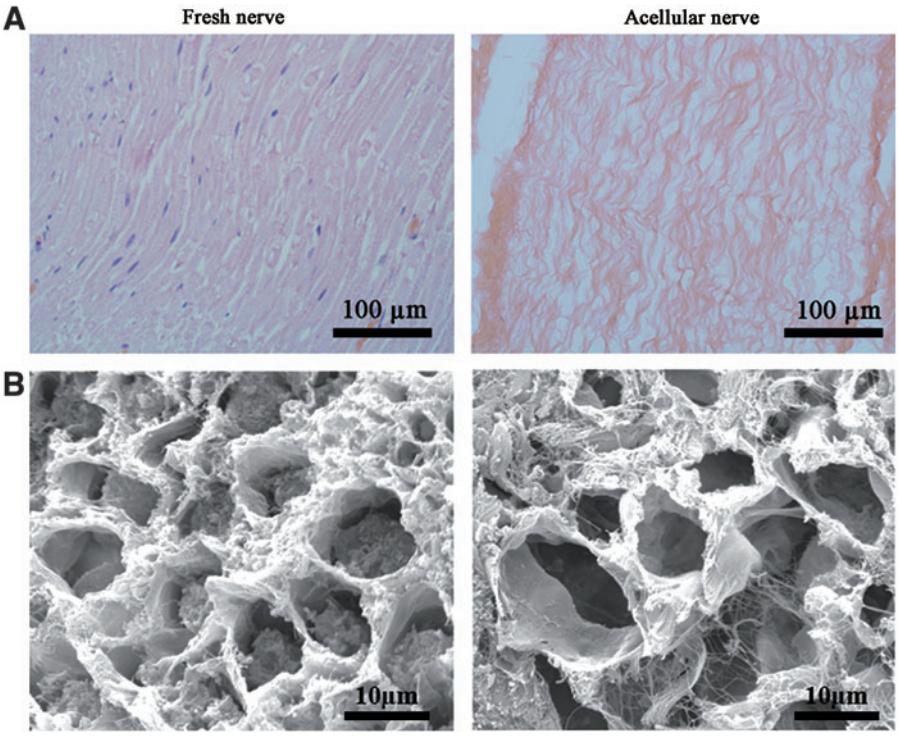

FIG. 1. Morphological observations of the acellular nerves. **(A)** A longitudinal section of the fresh nerve and acellular nerve by hematoxylin and eosin (H&E) staining. **(B)** Scanning electron microscopy images of the fresh nerve and acellular nerve. Compared with the fresh nerve, the components within cells, the myelin and the axon have been removed, whereas the endoneurial basal laminae remain intact. Color images available online at www.liebertpub.com/tea

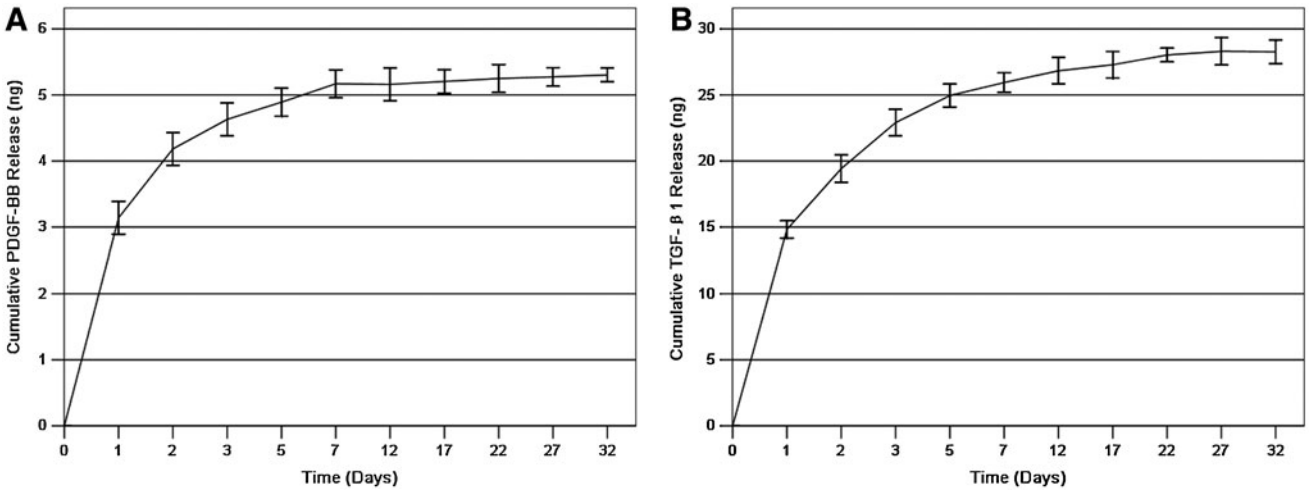

FIG. 2. The cumulative *in vitro* release of **(A)** platelet-derived growth factor (PDGF)-BB and **(B)** transforming growth factor-β1 (TGF-β1) from platelet-rich plasma (PRP) gels after leaching in phosphate-buffered saline (mean ± standard deviation [SD]; $n = 3$ for one batch). Both gels show a burst release of approximately 24 h, with a subsequent gradual release rate for 7 days.

fibroblasts, were present within the acellular nerve grafts. The alignment of fascicles and fibers was similar to that in the nerve before chemical extraction. Ultrastructural analysis by electron microscope imaging showed that after chemical extraction, the axons and myelin sheath were removed; whereas the basal lamina, collagen fibers, and endoneurial basal lamina were preserved and remained intact (Fig. 1).

Characterization of the PRP

The bio-effect of PRP is based on the premise that the large number of platelets in PRP release large quantities of growth factors. The growth factors released in the PRP were the result of platelet α-granule activation.[30] The average whole-blood platelet count ($n = 8$) was $478.12 \pm 102.36 \times 10^6$/mL, and the average PRP and PPP platelet counts ($n = 8$) were $3221.34 \pm 1016.32 \times 10^6$ and $25.25 \pm 13.68 \times 10^6$/mL, respectively. These platelet concentrations represented 6.74- and 0.053-fold increases, respectively, compared with the original platelet count. To test the duration of sustained growth factor release from PRP *in vitro*, ELISA kits were used to measure the concentrations of PDGF-BB and TGF-β1 released into PBS over 30 days. From the cumulative curve, there was an initial burst of PDGF-BB and TGF-β1 during the first 24 h. More than 50% of the PDGF-BB and TGF-β1 was released within the first day. After 24 h, the release rate was almost constant for 7 days followed by a slow release of the remaining growth factors over the next 25 days (Fig. 2). These results show that the release of PDGF-BB and TGF-β1 from PRP gels can be gradual *in vitro*.

Intra-operative view of implantation

The right sciatic nerves of all of the animals were carefully exposed at 12 weeks after grafting (Supplementary Fig. S1 shows macroscopic images of a sciatic nerve at an implantation site; Supplementary Data are available online at www.liebertpub.com/tea). We did not observe swelling, deformation, or breakage of the implants. No gross inflammatory reactions were observed in the peripheral nerve tissues, indicating the satisfactory biocompatibility of the implants.

Motor function assessment

The recovery of locomotive function in rats was assessed by calculating the SFI. The SFI varies from 0 to −100, with 0 corresponding to normal function and −100 corresponding to complete dysfunction. The four groups displayed a time-dependent increase in SFI values due to partial functional recovery (Fig. 3). In the first postoperative evaluation (4 weeks), the SFI value for all animals decreased dramatically to the lowest level with no obvious difference. The

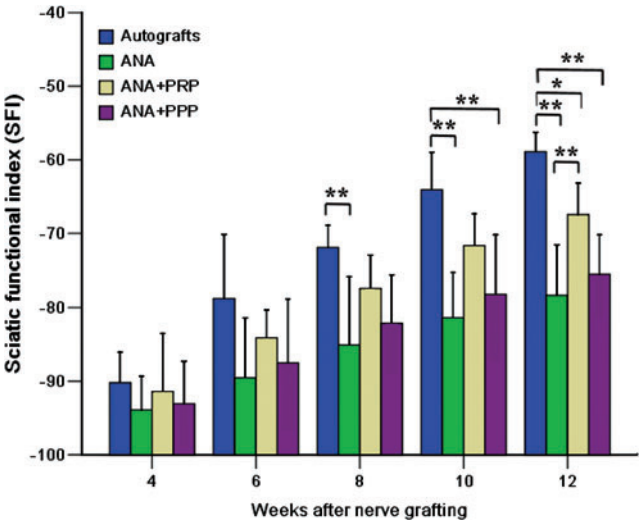

FIG. 3. A plot showing the sciatic functional index (SFI) evolution of the four grafted groups at 4, 6, 8, 10, and 12 weeks after nerve grafting. $n = 8$ for each group. $^*p < 0.05$, $^{**}p < 0.01$. Color images available online at www.liebertpub.com/tea

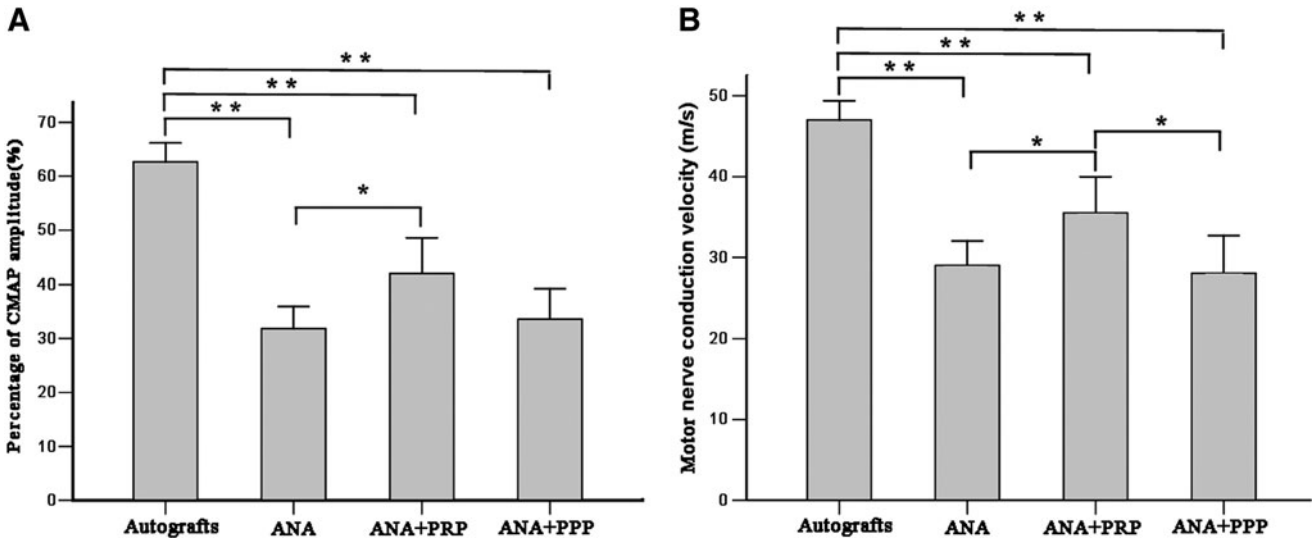

FIG. 4. Representative compound muscle action potential (CMAP) recordings for the four groups at 12 weeks after nerve grafting. **(A)** Histograms showing the CMAP recovery ratio and **(B)** motor nerve conduction velocity detected at the injured side. Error bars correspond to mean ± SD ($n = 8$ for each group). *$p < 0.05$, **$p < 0.01$.

SFI values improved substantially after the sixth week, indicating that some regenerated axons had passed through the nerve graft and into the target tissue. The footprints from the autograft group showed the greatest improvement, whereas the other groups improved only slightly. After 10 weeks, the SFI level for the autograft group was significantly higher than that of the ANA and ANA + PRP groups ($p < 0.01$). At 12 weeks, the SFI level of the autograft group was significantly higher than that of the other three groups, whereas the SFI level of the ANA + PRP group was also higher than that of the ANA group ($p < 0.01$).

To determine whether functional reinnervation occurred, an electrophysiological assessment was performed (Fig. 4). The percentage of the CMAP amplitude between the injured side and the contralateral uninjured side was calculated for the different groups. The percentage of CMAP amplitude was significantly higher for the autograft group than for any other group ($p < 0.01$), but it was also larger for the ANA + PRP group than for the ANA group ($p < 0.05$). The highest MCV value was observed for the autograft group, followed by the ANA + PRP group. The MCV value was significantly higher in the ANA + PRP group relative to the ANA and ANA + PPP groups ($p < 0.05$).

Histological analysis of the regenerated nerves

Newly formed nerves from each group were isolated and subjected to histological section staining of the distal implants at week 12 after nerve grafting. Longitudinal sections of the nerves were first stained by H&E (Fig. 5A). Newly formed nerves with linearly ordered structures were observed for all groups. No inflammatory reactions occurred around the regenerated nerves. However, the autograft and ANA + PRP groups provided more newly formed nerves and more correctly ordered linear guidance for growth compared with the other groups.

Axonal regeneration was investigated by staining NF-positive axons at the injured site (Fig. 5B). S-100 staining was performed to investigate the regeneration of SCs in the grafts (Fig. 5C). The statistical analysis indicated that both the autograft and ANA + PRP groups exhibited significantly higher percentages of NF-positive areas compared with the ANA and ANA + PPP groups at week 12 after nerve grafting ($p < 0.01$). The percentage of NF-positive areas was not significantly different between the autograft and ANA + PRP groups ($p > 0.05$) (Fig. 5D). The percentage of the S-100-positive stained area was statistically analyzed (Fig. 5E). The ANA + PRP group showed the highest percentage of S-100-positive stained area among the four groups. The autograft and ANA + PRP groups showed significantly more improvement in S-100 expression and SCs regeneration compared with the ANA and ANA + PPP groups ($p < 0.05$).

Remyelination of nerves

Nerve remyelination was compared among the groups by staining with toluidine blue (Fig. 6A) and by a transmission electron microscopic examination of the middle implants (Fig. 6B). Nerve fibers from the autograft and ANA + PRP groups were more closely and regularly arranged, with a larger diameter than those from the other groups. The ANA and ANA + PPP groups regenerated very few myelinated fibers distally and appeared to have more debris present. This result was in striking contrast to the autograft and ANA + PRP groups, in which there were abundant myelinated fibers. The number and diameter of remyelinated axons were statistically evaluated (Fig. 6C, D). At week 12 after nerve grafting, the autograft group had the greatest number and diameter of myelinated axons, followed by the ANA + PRP, ANA + PPP, and ANA groups. The autograft and ANA + PRP groups had significantly more axons and myelinated axons with larger diameters than the ANA group ($p < 0.05$). The thickness of the new myelin sheath was measured (Fig. 6E). The myelin thickness was significantly larger for the autograft group compared with the ANA and ANA + PPP groups ($p < 0.01$); however, no significant

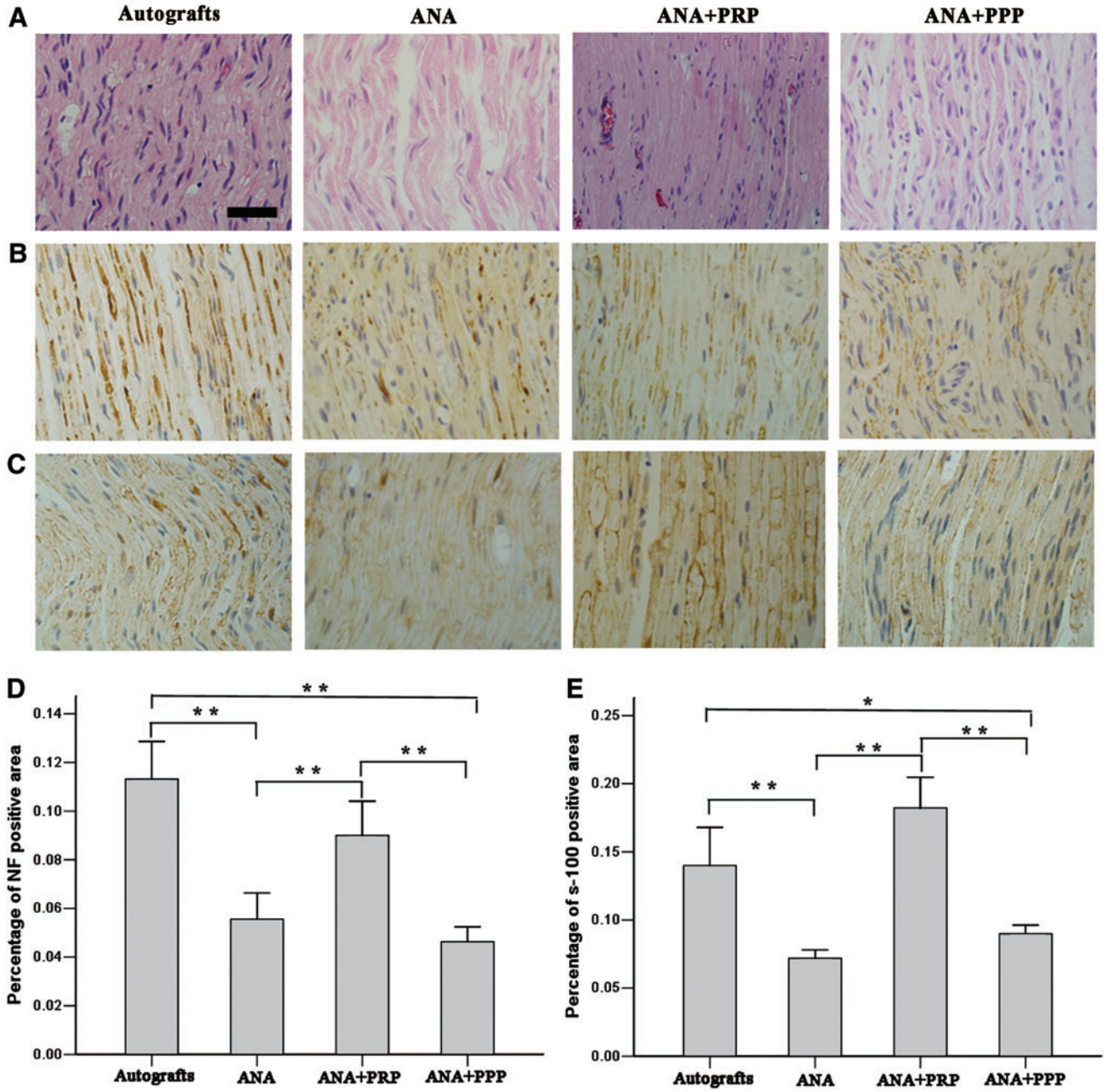

FIG. 5. Longitudinal sections of the regenerated nerve tissues and histological analysis for the four groups at week 12 after nerve grafting. **(A)** The longitudinal sections of the segments distal to the nerve grafts analyzed by H&E staining. **(B)** Immunostaining with anti-neurofilament antibody in longitudinal sections. **(C)** Immunostaining for the Schwann cell marker S-100 in the longitudinal sections. **(D)** Statistical analysis of the neurofilament-positive area for each group. **(E)** Statistical analysis for the S-100-positive area for each group. There were significant increases in the numbers of positively stained neurofilaments and S-100 for the autografts and acellular nerve allograft (ANA) + PRP groups but not for the ANA and ANA + platelet-poor plasma (PPP) groups. Error bars correspond to mean ± SD ($n = 8$ for each group). *$p < 0.05$, **$p < 0.01$. Scale bar = 50 μm. Color images available online at www.liebertpub.com/tea

difference was observed with regard to the ANA + PRP group ($p > 0.05$). The G-ratio was not significantly different among the groups (Fig. 6F).

RT-PCR analysis of gene expression

The four grafted groups were subjected to qRT-PCR to examine the mRNA levels of neurotrophic factor and nerve regeneration-related genes of the implant (Fig. 7). For qRT-PCR analysis, the dissociation of PCR constantly produced a single peak for each gene, indicating the presence of a unique product of each PCR primer. Both NGF and GDNF were significantly upregulated in both the autograft group and the ANA + PRP group compared with the other two groups ($p < 0.01$). There were no significant differences between the autograft and ANA + PRP groups in terms of

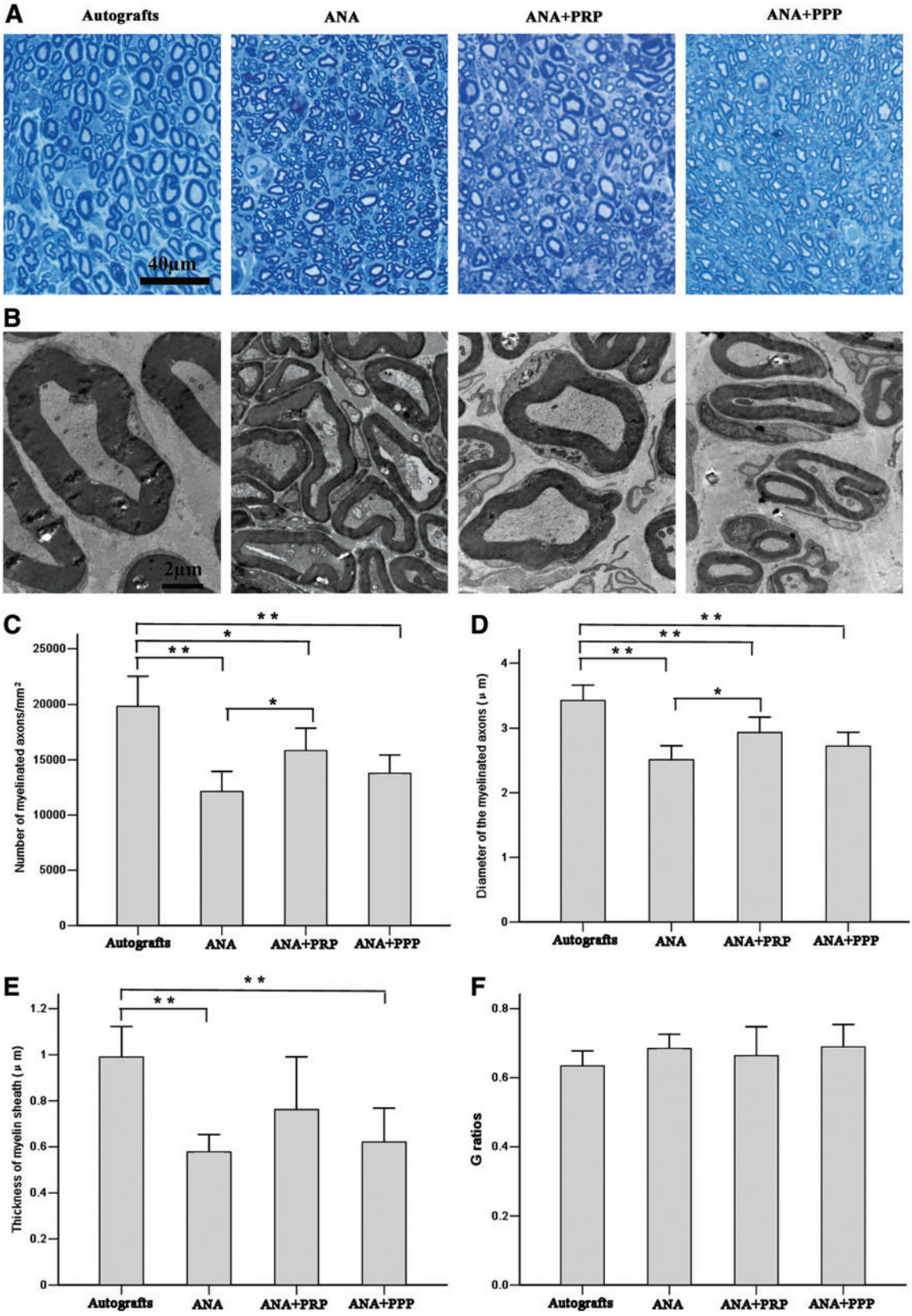

FIG. 6. Transverse sections of the midpoint of the harvested grafts from the four groups at week 12 after nerve grafting. **(A)** Staining with toluidine blue shows the regenerated axons. The autografts and the ANA + PRP group appear to have more regenerating nerve fibers than the other two groups. **(B)** Transmission electron micrographs demonstrate an increased amount of axon bundling and myelination in the autograft and ANA + PRP groups compared with the ANA and ANA + PPP groups. Comparisons of **(C)** the density, **(D)** axonal diameter, **(E)** thickness of the myelin sheaths, and **(F)** G ratios of the myelinated nerve fibers. Error bars correspond to mean ± SD ($n = 8$ for each group). $^{*}p < 0.05$, $^{**}p < 0.01$. Color images available online at www.liebertpub.com/tea

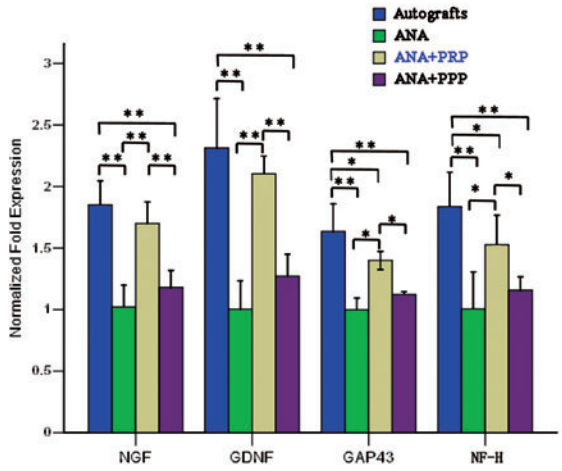

FIG. 7. The mRNA expression for nerve growth factor (NGF), glial-derived growth factor (GDNF), growth-associated protein 43 (GAP43), and neurofilament heavy (NF-H), as measured by quantitative real-time polymerase chain reaction (qRT-PCR), in the regenerating nerves taken from the four groups at 12 weeks after nerve grafting. The mRNA expression was calculated by the $2^{-\Delta\Delta CT}$ method using GDPHA as the reference gene. The relative mRNA levels were represented as the ratios by comparing the expression of each group with that of the ANA group (designated as 1). $n=4$ for each group, $^{*}p<0.05$, $^{**}p<0.01$. Color images available online at www.liebertpub.com/tea

NGF and GNDF gene expression ($p>0.05$). The highest mRNA levels for GAP43 and NF-H were observed in the autografts, followed by the ANA + PRP group. The lowest GAP43 and NF-H mRNA levels were observed in the ANA and ANA + PPP groups.

Examination of the triceps surae muscles

At postoperative week 12, the experimental triceps surae muscles exhibited gross atrophy compared with the contralateral controls (Supplementary Fig. S2). The tension percentage for the triceps surae muscles in the autograft group was 71.31% ± 8.39%, which was significantly higher than the values recorded for the ANA, ANA + PRP, and ANA + PPP groups (40.58% ± 6.10%, 56.64% ± 7.19%, and 42.98% ± 7.15%, respectively) ($p<0.05$). The tension percentage of the triceps surae muscles in the ANA + PRP group was significantly higher than that of the ANA and ANA + PPP groups ($p<0.05$). The target muscle morphometry was revealed by Masson trichrome staining at 12 months postsurgery (Fig. 8A). AChE staining of motor end plate units on longitudinal and frozen sections of target muscle (Fig. 8B) further indicated the attenuation of target muscle atrophy in the ANA + PRP and autograft groups because of the enhanced target reinnervation achieved after the repair of the injured sciatic nerves. In the ANA group, the motor endplates were hardly present and showed serious atrophy. Morphometric analysis

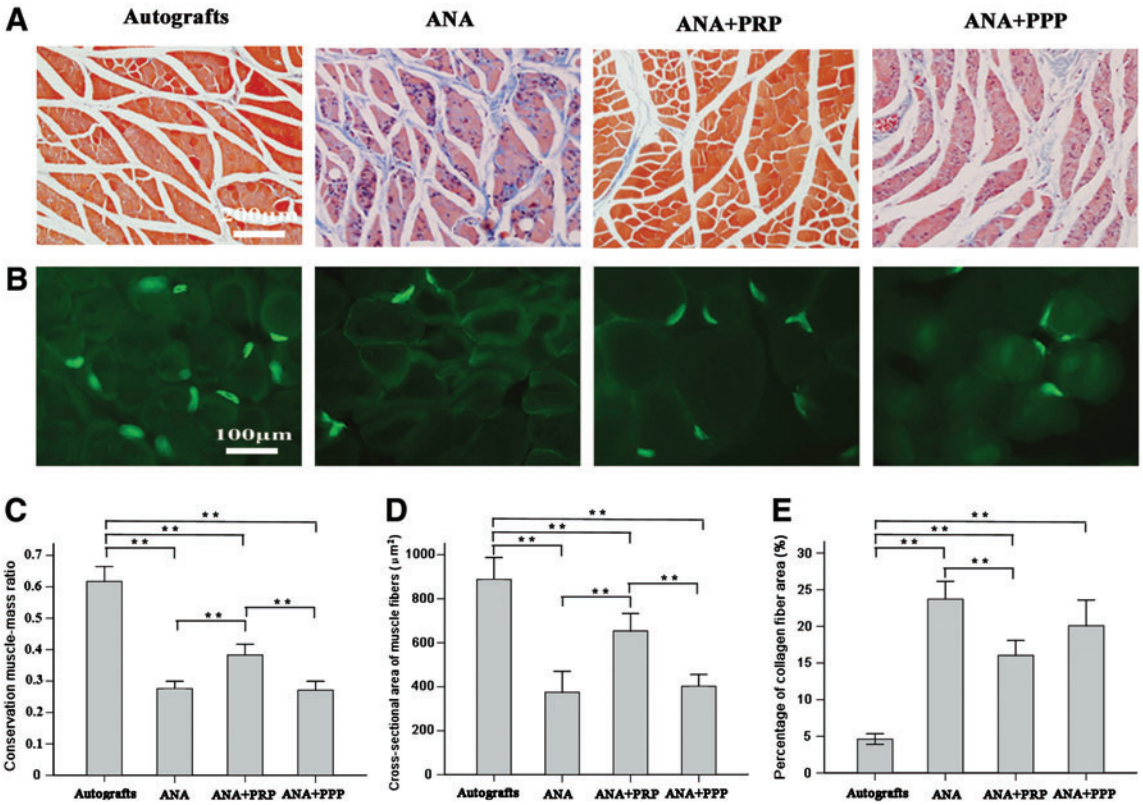

FIG. 8. Light micrographs of **(A)** Masson trichrome staining of transverse sections of the triceps surae muscles and **(B)** cholinesterase staining of the motor endplate on longitudinal sections of the triceps surae muscles from the sides of the rats that underwent operation, recorded at 12 weeks after nerve grafting. Histograms showing **(C)** conservation muscle–mass ratio, **(D)** cross-sectional area of the muscle fibers, and **(E)** average percentage of collagen fiber area for the triceps surae muscle samples from the sides that underwent the operation. Error bars correspond to mean ± SD ($n=8$ for each group). $^{*}p<0.05$, $^{**}p<0.01$. Color images available online at www.liebertpub.com/tea

enabled a quantitative comparison in terms of the target muscle-associated parameter (Fig. 8C–E). The wet weight ratio (injured side/contralateral uninjured side) of the autograft gastrocnemius muscle was greatest among all of the groups. In addition, the ANA + PRP group was heavier than either the ANA or ANA + PPP groups ($p < 0.01$) (Fig. 8C). The delineation and reinnervation of muscle were assessed based on muscle fiber type and cross-sectional area evaluation to provide an in-depth understanding of the muscle physiology during recovery. The autograft and ANA + PRP groups had larger muscle fiber areas than the ANA group or ANA + PRP groups ($p < 0.01$) (Fig. 8D). The average percentage of collagen fiber area in the target muscle on the injured side was significantly larger in the ANA group than in the autograft and ANA + PRP groups ($p < 0.01$) (Fig. 8E).

Discussion

Our study demonstrates that ANAs present a biomimetic three-dimensional architecture which maintains the natural physical characteristics of basal lamina tubes and elicits minimal immune responses through a chemical extraction protocol. These characteristics enable ANAs to support axonal regeneration and muscle reinnervation without exhibiting the overt signs of rejection or infection.[7] However, acellular grafts cannot provide full functional recovery comparable to nerve autografts due to the lack of an appropriate microenvironment for axonal regeneration.[22] Nerve regeneration and target reinnervation are complex processes involving the appropriate microenvironment that pertains to the neuron, the growth, and the target. To achieve better regeneration, we hypothesized that including PRP at the acellular nerve repair site to mimic the native nerve microenvironment can accelerate axon regeneration.

PRP has been used clinically in humans since the 1970s for its healing properties attributed to autologous growth factors and secretory proteins that may enhance the healing process on a cellular level. Furthermore, PRP enhances the recruitment, proliferation, and differentiation of cells involved in tissue regeneration.[31] Three major storage compartments in platelets are alpha granules, dense granules, and lysosomes. The majority of the platelet substances are contained in alpha granules. On activation, platelets from PRP release their granular contents into the surrounding environment. The platelet alpha granules are abundant and contain many of the growth factors responsible for the initiation and maintenance of the regeneration response.[32] Among the bioactive molecules stored and released from platelets dense granules are catecholamines, histamine, serotonin, ADP, ATP, calcium ions, and dopamine, which are active in vasoconstriction, increasing capillary permeability, attracting and activating macrophages, and enhancing tissue modulation during regenerative processes. These nongrowth factors molecules also have fundamental effects on the biologic aspects of wound healing and tissue repair.[33]

In our study, we selected rat sciatic nerve defects measuring 15 mm in length for reconstruction with various nerve grafts because a relatively large gap was necessary when studying the rat to determine the relative effectiveness of nerve regeneration among the groups. To explore eligible nerve substitutes, the effectiveness of regeneration for the autograft, ANA, ANA + PRP, and ANA + PPP groups was evaluated at 12 weeks post-transplantation. First, the recovery of motor function in the injured hindlimb, as indexed by the SFI value, showed that the repair effect for the ANA + PRP group was almost the same as the autograft group but was far superior to that of the ANA and ANA + PPP groups. The neural electrophysiology provided clear evidence that the functional recovery in the ANA + PRP group was significantly better than that of the ANA and ANA + PRP groups, although it was not as good as the functional recovery of the autograft group. Histological evaluation showed that the ANA + PRP group provided better support for nerve regeneration. More axons successfully crossed the repair site from the proximal to the distal segment in the ANA + PRP and autograft groups. In terms of both the qualitative and quantitative aspects, the ANA + PRP group exhibited better reconstruction of the regenerated nerve and the gastrocnemius target muscle than either the ANA or ANA + PPP groups. These data demonstrate that the topical application of PRP enhances peripheral nerve regeneration, but the effect was more effective in improving reconstruction of the target muscle rather than increasing myelination of newly regenerated axons.

Successful mammalian peripheral nerve regeneration after nerve injury depends on the activation of SCs and their supportive role in the production of neurotrophic and neurotropic factors (such as NGF or GDNF), which enhance neural recovery.[30] In our study, the ANA + PRP group showed the highest percentage of SCs markers in terms of the S-100-positive stained area among the four groups. This finding may indicate that PRP contains a concentrated suspension of growth factors that can promote the proliferation of SCs *in vivo* compared with the nontreated groups. The proliferation of SCs *in vivo* can appropriately secrete various neurotrophic factors, such as NGF, GDNF, brain-derived neurotrophic factor, and ciliary neurotrophic factor, among others, which have been previously reported to aid in the support and maintenance of peripheral nervous system axons.[34] In the present study, compared with the ANA and ANA + PPP groups, the mRNA levels of NGF and GDNF, which are important neurotrophic factors in nerve regeneration, were similar between the ANA + PRP group and the autograft group. NGF and GDNF have been shown to improve neuronal survival and nerve regeneration in nerve injuries.[27,35] These factors may have partly originated from the proliferation of SCs, which were activated in the neurotrophic milieu to enhance peripheral nerve regeneration. These findings might contribute to an explanation for the underlying mechanism of PRP action in enhancing axonal outgrowth by promoting the proliferation of SCs and upregulating the expression of NGF and GDNF within the regenerating nerves.[36]

Our study shows that more axons successfully grow through the ANA + PRP to reach the distal stumps to reinnervate the target muscle compared with the ANA containing no bioactive agents (PPP). These results suggest that growth factors released from the PRP, rather than serum proteins, may play a crucial role in nerve regeneration. The introduction of PRP containing various growth factors into acellular nerve grafts might contribute to the establishment of a native-like microenvironment for nerve regeneration in a similar manner to autografts. The physical stimulus of the PRP also might provide cues for SCs,

enhancing neural tube formation and the activation of neurotrophic factors that accelerate axoplasm production.

In this study, autologous PRP was prepared after the two-step centrifugation of blood obtained from rats without the use of commercial kits. PRP was selected as the active component with ANAs for the promotion of nerve regeneration, because PRP offers the advantage of availability at the point of care in a simple and relatively inexpensive manner in contrast to the more complicated processes of gathering stem cells or recombinant growth factors. Some reports demonstrate that the local application of PDGB-BB and/or TGF-β1 as a single agent enhances nerve regeneration or regulates the proliferation and differentiation of SCs.[37–41] Neurons that express PDGF receptors have been proved to be a mitogen and survival factor for SCs with trophic activity on neurons. In addition, augmented PDGF expression in peripheral neurons has been found after peripheral nerve injury, suggesting a positive role in peripheral nerve regeneration.[37,42] TGF-β1 plays a central role in the regulation of SCs proliferation and differentiation and is essential for the neurotrophic effects of several neurotrophic factors.[39,40] Our study showed that PRP has the ability to release PDGF-BB and TGF-β1 *in vitro* over relatively short time points. The release profile was characterized by a prominent burst of release within the first few days, followed by a period of gradual release over the subsequent weeks. However, PRP can release growth factors that maintain their activity over a relatively short period. PRP releases growth factors quickly and appears to be insufficient for peripheral nerve regeneration over long periods of time. This shortcoming explains why the ANA + PRP group showed slightly inferior functional recovery compared with the autograft group with regard to some of the studied parameters. Future studies should attempt to prolong the duration of growth factor release to facilitate improved nerve repair. Another limitation of the study is for how long PRP keep releasing growth factors *in vivo* and how much of the growth factors from the gel are released to the ANAs. This could be our proposed future goal.

PRP is an autologous preparation, utilizing the patient's own blood in a significantly small quantity. For this reason, it is safe and there have been no published references related to the risk of infections, disease transmission, immunogenic reactions, or any other adverse effects that exist with allografts or xenografts. What is more, the preparation of PRP is rapid, simple, convenient, and economical. Although no undesirable effects have been reported in the many clinical cases subjected to PRP therapy, similar to what might happen in other cell or biological product-based therapies, hypotheses with regard to the over-expression of growth factors and their receptors related to tumor and dysplastic tissues have been postulated.[43]

As we know, our study is the first which reports that ANAs accompanied by PRP can enhance the repair capacity of peripheral nerve injuries. The ANA + PRP group showed promise for rescuing muscle atrophy and stimulating myelinated axon regeneration, and the extent of nerve repair observed was nearly the same as that exhibited by the autograft group. Growth factors, such as PDGF-BB and TGF-β1 released from the PRP, rather than serum proteins, may play a crucial role in nerve regeneration. Acellular grafts incorporating PRP as tissue-engineered scaffolds represent promising treatments for the repair of peripheral nerve large defects and the promotion of nerve regeneration, providing an experimental basis for future clinical applications. This procedure can be easily adapted to most clinical settings with minimal infrastructure so that many patients can benefit from this cellular therapy.

Acknowledgments

This work was supported by grants from the National High Technology Research and Development Program of China (863 Program, No. 2012AA020507), the National Basic Research Program of China (973 Program, No. 2014CB542201), National Natural Science Foundation of China (No.81401804), Medical Scientific Research Foundation of Guangdong Province (No. B2014119) and the 985 program of Sun Yat-sen University (No. 90035-3283312).

Disclosure Statement

The authors declare that no competing financial interests exist.

References

1. Huang, W., Begum, R., Barber, T., Ibba, V., Tee, N.C., Hussain, M., Arastoo, M., Yang, Q., Robson, L.G., Lesage, S., Gheysens, T., Skaer, N.J., Knight, D.P., and Priestley, J.V. Regenerative potential of silk conduits in repair of peripheral nerve injury in adult rats. Biomaterials **33,** 59, 2012.
2. Shen, C.C., Yang, Y.C., and Liu, B.S. Peripheral nerve repair of transplanted undifferentiated adipose tissue-derived stem cells in a biodegradable reinforced nerve conduit. J Biomed Mater Res A **100,** 48, 2012.
3. Kim, B.S., Yoo, J.J., and Atala, A. Peripheral nerve regeneration using acellular nerve grafts. J Biomed Mater Res A **68,** 201, 2004.
4. Yang, L.M., Liu, X.L., Zhu, Q.T., Zhang, Y., Xi, T.F., Hu, J., He, C.F., and Jiang, L. Human peripheral nerve-derived scaffold for tissue-engineered nerve grafts: histology and biocompatibility analysis. J Biomed Mater Res B Appl Biomater **96,** 25, 2011.
5. Giusti, G., Willems, W.F., Kremer, T., Friedrich, P.F., Bishop, A.T., and Shin, A.Y. Return of motor function after segmental nerve loss in a rat model: comparison of autogenous nerve graft, collagen conduit, and processed allograft (AxoGen). J Bone Joint Surg Am **94,** 410, 2012.
6. Saheb-Al-Zamani, M., Yan, Y., Farber, S.J., Hunter, D.A., Newton, P., Wood, M.D., Stewart, S.A., Johnson, P.J., and Mackinnon, S.E. Limited regeneration in long acellular nerve allografts is associated with increased Schwann cell senescence. Exp Neurol 247C **165,** 2013.
7. Moore, A.M., MacEwan, M., Santosa, K.B., Chenard, K.E., Ray, W.Z., Hunter, D.A., Mackinnon, S.E., and Johnson, P.J. Acellular nerve allografts in peripheral nerve regeneration: a comparative study. Muscle Nerve **44,** 221, 2011.
8. Gu, X., Ding, F., Yang, Y., and Liu, J. Construction of tissue engineered nerve grafts and their application in peripheral nerve regeneration. Prog Neurobiol **93,** 204, 2011.
9. Jesuraj, N.J., Santosa, K.B., Macewan, M.R., Moore, A.M., Kasukurthi, R., Ray, W.Z., Flagg, E.R., Hunter, D.A., Borschel, G.H., Johnson, P.J., Mackinnon, S.E., and Sakiyama-Elbert, S.E. Schwann cells seeded in acellular nerve grafts improve functional recovery. Muscle Nerve **49,** 267, 2014.

10. Tomita, K., Madura, T., Sakai, Y., Yano, K., Terenghi, G., and Hosokawa, K. Glial differentiation of human adipose-derived stem cells: implications for cell-based transplantation therapy. Neuroscience **236,** 55, 2013.
11. de Ruiter, G.C., Malessy, M.J., Yaszemski, M.J., Windebank, A.J., and Spinner, R.J. Designing ideal conduits for peripheral nerve repair. Neurosurg Focus **26,** E5, 2009.
12. Bell, J.H., and Haycock, J.W. Next generation nerve guides: materials, fabrication, growth factors, and cell delivery. Tissue Eng Part B Rev **18,** 116, 2012.
13. Scheib, J., and Hoke, A. Advances in peripheral nerve regeneration. Nat Rev Neurol **9,** 668, 2013.
14. Kotsovilis, S., Markou, N., Pepelassi, E., and Nikolidakis, D. The adjunctive use of platelet-rich plasma in the therapy of periodontal intraosseous defects: a systematic review. J Periodontal Res **45,** 428, 2010.
15. Rutkowski, J.L., Thomas, J.M., Bering, C.L., Speicher, J.L., Radio, N.M., Smith, D.M., and Johnson, D.A. Analysis of a rapid, simple, and inexpensive technique used to obtain platelet-rich plasma for use in clinical practice. J Oral Implantol **34,** 25, 2008.
16. Andia, I., Sanchez, M., and Maffulli, N. Joint pathology and platelet-rich plasma therapies. Expert Opin Biol Ther **12,** 7, 2012.
17. Arora, N.S., Ramanayake, T., Ren, Y.F., and Romanos, G.E. Platelet-rich plasma: a literature review. Implant Dent **18,** 303, 2009.
18. Nguyen, R.T., Borg-Stein, J., and McInnis, K. Applications of platelet-rich plasma in musculoskeletal and sports medicine: an evidence-based approach. PM R 3 **226,** 2011.
19. Cho, H.H., Jang, S., Lee, S.C., Jeong, H.S., Park, J.S., Han, J.Y., Lee, K.H., and Cho, Y.B. Effect of neural-induced mesenchymal stem cells and platelet-rich plasma on facial nerve regeneration in an acute nerve injury model. Laryngoscope **120,** 907, 2010.
20. Zheng, C., Zhu, Q., Liu, X., Huang, X., He, C., Jiang, L., Quan, D., Zhou, X., and Zhu, Z. Effect of platelet-rich plasma (PRP) concentration on proliferation, neurotrophic function and migration of Schwann cells *in vitro*. J Tissue Eng Regen Med 2013.
21. Sondell, M., Lundborg, G., and Kanje, M. Regeneration of the rat sciatic nerve into allografts made acellular through chemical extraction. Brain Res **795,** 44, 1998.
22. Wang, D., Liu, X.L., Zhu, J.K., Hu, J., Jiang, L., Zhang, Y., Yang, L.M., Wang, H.G., Zhu, Q.T., Yi, J.H., and Xi, T.F. Repairing large radial nerve defects by acellular nerve allografts seeded with autologous bone marrow stromal cells in a monkey model. J Neurotrauma **27,** 1935, 2010.
23. Yamaguchi, R., Terashima, H., Yoneyama, S., Tadano, S., and Ohkohchi, N. Effects of platelet-rich plasma on intestinal anastomotic healing in rats: PRP concentration is a key factor. J Surg Res **173,** 258, 2012.
24. Bain, J.R., Mackinnon, S.E., and Hunter, D.A. Functional evaluation of complete sciatic, peroneal, and posterior tibial nerve lesions in the rat. Plast Reconstr Surg **83,** 129, 1989.
25. Amado, S., Simoes, M.J., Armada, D.S.P., Luis, A.L., Shirosaki, Y., Lopes, M.A., Santos, J.D., Fregnan, F., Gambarotta, G., Raimondo, S., Fornaro, M., Veloso, A.P., Varejao, A.S., Mauricio, A.C., and Geuna, S. Use of hybrid chitosan membranes and N1E-115 cells for promoting nerve regeneration in an axonotmesis rat model. Biomaterials **29,** 4409, 2008.
26. Bozkurt, A., Lassner, F., O'Dey, D., Deumens, R., Bocker, A., Schwendt, T., Janzen, C., Suschek, C.V., Tolba, R., Kobayashi, E., Sellhaus, B., Tholl, S., Eummelen, L., Schugner, F., Damink, L.O., Weis, J., Brook, G.A., and Pallua, N. The role of microstructured and interconnected pore channels in a collagen-based nerve guide on axonal regeneration in peripheral nerves. Biomaterials **33,** 1363, 2012.
27. Tang, S., Zhu, J., Xu, Y., Xiang, A.P., Jiang, M.H., and Quan, D. The effects of gradients of nerve growth factor immobilized PCLA scaffolds on neurite outgrowth *in vitro* and peripheral nerve regeneration in rats. Biomaterials **34,** 7086, 2013.
28. Li, Z., Peng, J., Wang, G., Yang, Q., Yu, H., Guo, Q., Wang, A., Zhao, B., and Lu, S. Effects of local release of hepatocyte growth factor on peripheral nerve regeneration in acellular nerve grafts. Exp Neurol **214,** 47, 2008.
29. di Summa, P.G., Kingham, P.J., Raffoul, W., Wiberg, M., Terenghi, G., and Kalbermatten, D.F. Adipose-derived stem cells enhance peripheral nerve regeneration. J Plast Reconstr Aesthet Surg **63,** 1544, 2010.
30. Elgazzar, R.F., Mutabagani, M.A., Abdelaal, S.E., and Sadakah, A.A. Platelet rich plasma may enhance peripheral nerve regeneration after cyanoacrylate reanastomosis: a controlled blind study on rats. Int J Oral Maxillofac Surg **37,** 748, 2008.
31. Nurden, A.T. Platelets, inflammation and tissue regeneration. Thromb Haemost 105 Suppl 1, **S13,** 2011.
32. Sanchez-Gonzalez, D.J., Mendez-Bolaina, E., and Trejo-Bahena, N.I. Platelet-rich plasma peptides: key for regeneration. Int J Pept **2012,** 532519, 2012.
33. Qureshi, A.H., Chaoji, V., Maiguel, D., Faridi, M.H., Barth, C.J., Salem, S.M., Singhal, M., Stoub, D., Krastins, B., Ogihara, M., Zaki, M.J., and Gupta, V. Proteomic and phospho-proteomic profile of human platelets in basal, resting state: insights into integrin signaling. PLoS One **4,** e7627, 2009.
34. Santosa, K.B., Jesuraj, N.J., Viader, A., MacEwan, M., Newton, P., Hunter, D.A., Mackinnon, S.E., and Johnson, P.J. Nerve allografts supplemented with schwann cells overexpressing glial-cell-line-derived neurotrophic factor. Muscle Nerve **47,** 213, 2013.
35. Chu, T.H., Wang, L., Guo, A., Chan, V.W., Wong, C.W., and Wu, W. GDNF-treated acellular nerve graft promotes motoneuron axon regeneration after implantation into cervical root avulsed spinal cord. Neuropathol Appl Neurobiol **38,** 681, 2012.
36. de Boer, R., Borntraeger, A., Knight, A.M., Hebert-Blouin, M.N., Spinner, R.J., Malessy, M.J., Yaszemski, M.J., and Windebank, A.J. Short- and long-term peripheral nerve regeneration using a poly-lactic-co-glycolic-acid scaffold containing nerve growth factor and glial cell line-derived neurotrophic factor releasing microspheres. J Biomed Mater Res A **100,** 2139, 2012.
37. Oya, T., Zhao, Y.L., Takagawa, K., Kawaguchi, M., Shirakawa, K., Yamauchi, T., and Sasahara, M. Platelet-derived growth factor-b expression induced after rat peripheral nerve injuries. Glia **38,** 303, 2002.
38. Jiang, H., Qu, W., Li, Y., Zhong, W., and Zhang, W. Platelet-derived growth factors-bb and fibroblast growth factors-base induced proliferation of schwann cells in a 3D environment. Neurochem Res **38,** 346, 2013.
39. McLennan, I.S., and Koishi, K. The transforming growth factor-betas: multifaceted regulators of the development

and maintenance of skeletal muscles, motoneurons and Schwann cells. Int J Dev Biol **46,** 559, 2002.
40. Rosner, B.I., Hang, T., and Tranquillo, R.T. Schwann cell behavior in three-dimensional collagen gels: evidence for differential mechano-transduction and the influence of TGF-beta 1 in morphological polarization and differentiation. Exp Neurol **195,** 81, 2005.
41. Zhang, Y., Jin, Y., Nie, X., Wang, Y., Liu, P., Shen, N., and Guo, S. [Tissue engineering peripheral nerve with TGF-beta repair sciatic nerve defect]. Sheng Wu Yi Xue Gong Cheng Xue Za Zhi **24,** 394, 2007.
42. Eccleston, P.A., Funa, K., and Heldin, C.H. Expression of platelet-derived growth factor (PDGF) and PDGF alpha- and beta-receptors in the peripheral nervous system: an analysis of sciatic nerve and dorsal root ganglia. Dev Biol **155,** 459, 1993.
43. Albanese, A., Licata, M.E., Polizzi, B., and Campisi, G. Platelet-rich plasma (PRP) in dental and oral surgery: from the wound healing to bone regeneration. Immun Ageing **10,** 23, 2013.

Address correspondence to:
Xiaolin Liu, MD, PhD
Department of Orthopedic and Microsurgery
The First Affiliated Hospital
Sun Yat-sen University
58 Zhongshan Er Road
Guangzhou GD 510080
China

E-mail: gzxiaolinliu@hotmail.com

Qingtang Zhu, MD, PhD
Department of Orthopedic and Microsurgery
The First Affiliated Hospital
Sun Yat-sen University
58 Zhongshan Er Road
Guangzhou GD 510080
China

E-mail: qtzhu@qq.com

Received: November 30, 2013
Accepted: May 28, 2014
Online Publication Date: September 26, 2014